

Augmenting the performance of photovoltaic cell through surface coating of molybdenum disulphide

S. Prashanth^a, R. Rajasekar^{b,*}, V. K. Gobinath^c, G. Raja^d, K. Subha^e,
K. S. Manjunath^f

^aDepartment of Aeronautical Engineering, Excel Engineering College, Namakkal, Tamil Nadu, India – 637303

^bDepartment of Mechanical Engineering, Kongu Engineering College, Perundurai, Tamil Nadu, India - 638060,

^cDepartment of Mechatronics Engineering, Kongu Engineering College, Perundurai, Tamil Nadu, India - 638060

^dDepartment of Mechanical Engineering, Velalar college of Engineering and Technology, Erode, India – 638012

^eNanotechnology Research Center, SRMIST, Tamil Nadu, India – 603203

^fDepartment of Pharmacology, Saveetha Dental College (SDC), Saveetha Institute of Medical and Technical Science, Chennai, Tamil Nadu, India

The current investigation is focused on sol-gel grown molybdenum disulphide (MoS₂) as an anti-reflection coating (ARC) material to increase performance of photovoltaic solar cells. Four layers (C-I, C-II, C-III & C-IV) at different thickness of MoS₂ were deposited on polycrystalline solar substrate using spin coating technique. The effect of MoS₂ coated on morphological structure, optical and electrical properties and thermal behaviour of solar cell are investigated. The C-III layer coated solar cells demonstrated minimum reflectance of 12 % in the UV visible region (300 - 800 nm). The maximum power conversion efficiency (PCE) of 17.40 % (open environment source) and 19.23 % (closed controlled environment source) has been achieved at C-III layer coated solar cell. The C-III coated solar cell exhibited minimum cell temperature at 37.5 °C (open source) and 52.5 °C (closed source). The sol-gel developed MoS₂ exhibits the desirable properties to be an ARC material for improving the PCE of solar cells.

(Received January 31, 2021; Accepted April 2, 2021)

Keywords: Molybdenum disulphide, Spin coating, Power conversion efficiency

1. Introduction

Eco-friendly based energy is of great interest as it overcomes the environmental pollution caused by the fossil fuels [1, 2]. In recent years, solar energy has main impact on solving the energy crisis than the various renewable energy sources because it possesses maximum power conversion efficiency, limitless energy and environmental friendly. As seen there are many researchers focused on improving the power conversion efficiency of photovoltaic solar cells. The improvement of power conversion efficiency makes them cost effective than the other conventional energy resources [3]. The photovoltaic solar cells are produced using silicon and they are divided into monocrystalline and polycrystalline. Polycrystalline solar cells are more preferred than monocrystalline cells as they involves simple production processes and less cost [4]. The light rays from sun hits the surface of panel at a certain angle and it travels through protective layer of glass and reach the cell. As observed, all of the rays at glass surface are not transferred to cell, 8% to 10% of incident light is reflected from the surface [5]. The more reflection of light may induces optical loss in the production of electric power. The reduction of optical losses is a key process to maximize the efficiency of the solar cells [6].

*Corresponding author: rajasekar.cr@gmail.com

<https://doi.org/10.15251/CL.2021.184.161>

Anti-reflective coating (ARC) is used to minimize optical loss by applying on the surface of the solar panel. The ARC's helps to improve the short-circuit current (I_{sc}) and to maximize power conversion efficiency. Recent researchers focused on increasing the efficiency of the solar cell through different ARC materials such as SiO_2 , MgF_2 , TiO_2 , Si_3N_4 , ZrO_2 , Al_2O_3 , ZnO , Ta_2O_5 , HfO_2 , CeO_2 [2, 7-10] with appropriate coating methods. The light absorbing capability can be increased by using the materials possessing higher antireflective properties. Molybdenum sulphide (MoS_2) is identified as a potential antireflective material because of its minimum cost and availability. The anti-reflective properties and less toxicity make MoS_2 suitable for photovoltaic applications. MoS_2 is a semiconductor material possessing band gap of 1.8 eV, which makes them promising antireflective material in the field of visible-spectrum [11]. MoS_2 is one of the transition metal dichalcogenides, which is capable of trapping incident light with subsequent reduction in reflectivity on the surface of solar cell. The electrical, thermal and optical characteristics of photovoltaic solar cells can be enhanced while using MoS_2 thin-film layer. The thin-film ARCs have been deposited using different methods like spray pyrolysis, dip coating, spin coating, sputtering, pulsed laser deposition [12-15].

In the current research work, the investigation has been performed to analyse the influence of MoS_2 nano-layer as a front contact anti-reflective layer for improved light trapping of polycrystalline silicon solar cells. The MoS_2 nano-layers of ARCs were prepared by spin coating on the silicon solar cell surface. Structural, surface morphology, optical, electrical and temperature behaviour of MoS_2 nano-layers deposited on solar cells is analysed in detail.

2. Experimental part

2.1. Materials and chemicals

All chemical reagents are procured from Sigma Aldrich with high grade analytical level. The commercial available polycrystalline silicon solar cell (5.2 cm * 3.8 cm) were purchased from Vikram Solar, India.

2.2. MoS_2 preparation

Initially, the ammonium molybdate tetrahydrate ($(\text{NH}_4)_6\text{Mo}_7\text{O}_{24}\cdot 4\text{H}_2\text{O}$) of 0.2g was dissolved in deionized water of 0.8 litres followed by the addition of 0.4 g thioacetamide (CH_3CSNH_2) under constant stirring. There is a further addition of 0.05 g diethylenetriamine pentaacetic acid (Dtpa) in order to attain the brown sol under regular stirring for 2 hours. The obtained sol is placed in oven at 60 °C for 12 hours to form bronze gel and dried for two days. MoS_2 is formed by placing this xerogel in tube furnace under argon gas atmosphere flows at 170 sccm.

2.3. Deposition of MoS_2 on solar cells

The obtained MoS_2 is dissolved in ethanol (0.1g MoS_2 in 10 ml) to form sol solution which is to be continuously stirred for 1 hour at room temperature. Then the solution is subjected to sonication process for 10 min and stirred continuously under room temperature for 30 min. The substrates of the solar cells are cleaned using deionized water before coating. The spin coating method was employed to deposit the obtained sol solution on the substrates of polycrystalline silicon solar cells [16, 17]. These layers were deposited at a constant speed of 5000 rpm for 30 seconds. Deposition Parameters are shown in Table 1.

Table 1. MoS₂ deposition parameters

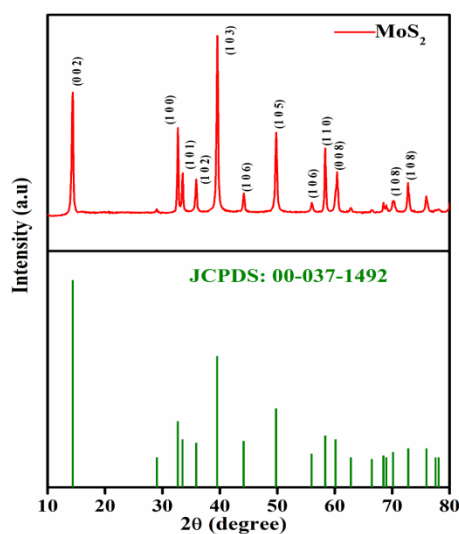
| Deposition Layers | Spin coating speed (rpm) | Time Duration (sec) | Layer Thickness (nm) | Drying Temperature (°C) |
|-------------------|--------------------------|---------------------|----------------------|-------------------------|
| C-I | 5000 | 30 | 215 | 110 |
| C-II | | | 428 | |
| C-III | | | 652 | |
| C-IV | | | 902 | |

2.4. Characterization techniques

The calcinated MoS₂ samples were analyzed using X-ray diffraction (XRD) technique to determine the properties of structure and degree of crystallinity. The morphology of the MoS₂ surface on the solar cells was examined using Atomic Force Microscopy (AFM). UV-Vis-NIR spectrophotometer was employed to determine the reflectance and transmittance properties of both coated and uncoated solar cells. The thickness of the MoS₂ coating and their surface morphology were interpreted using Field Emission Scanning Electron Microscopy (FE-SEM). Keithley 2450 source meter was used to monitor the current-voltage relationships of both uncoated and MoS₂ coated polycrystalline silicon solar cells. The four probe technique was used to determine the resistivity of the MoS₂ coated and uncoated solar cells. Thermal images are captured by infrared thermal imaging for the analyzing the temperature behavior of both uncoated and MoS₂ coated cells.

3. Results and discussion

The XRD pattern of calcinated MoS₂ samples at 900 °C is depicted in Fig. 1. As observed, it is clear that the obtained peaks are almost same as that of MoS₂ indexed structure with cubic crystal system (JCPDS file No.00-037-1492). The diffraction peaks obtained by MoS₂ sample are sharp, indicates the high degree of crystallinity. The Miller indices (002), (100), (101), (102), (103), (106), (105), (106), (110), (008) and (108) obtained are well indexed with the MoS₂ structure. The diffraction peaks position and the miller indices of synthesized MoS₂ are in accordance with the standard diffraction data (Fig. 1).

Fig. 1. XRD pattern of MoS₂.

The FESEM images depicting surface morphology and cross sectional images of the MoS₂ coated polycrystalline solar cells are shown in Fig. 2 & 3 (a – d). The structure and morphology of anti-reflective layers depends on the parameters including spinning speed, spinning speed, coating layers and heating temperatures after coating. Compact, dense and partial pinhole morphology can be observed from the figure. The grains appear larger as they are crystallized and merged. Thicknesses of the MoS₂ thin films examined by the cross-section FESEM images were 215, 428, 652 and 902 nm respectively. It is clear from FESEM images that while increasing the layers of MoS₂ deposition, the thickness of the film increases which in turn increases the grain size [18].

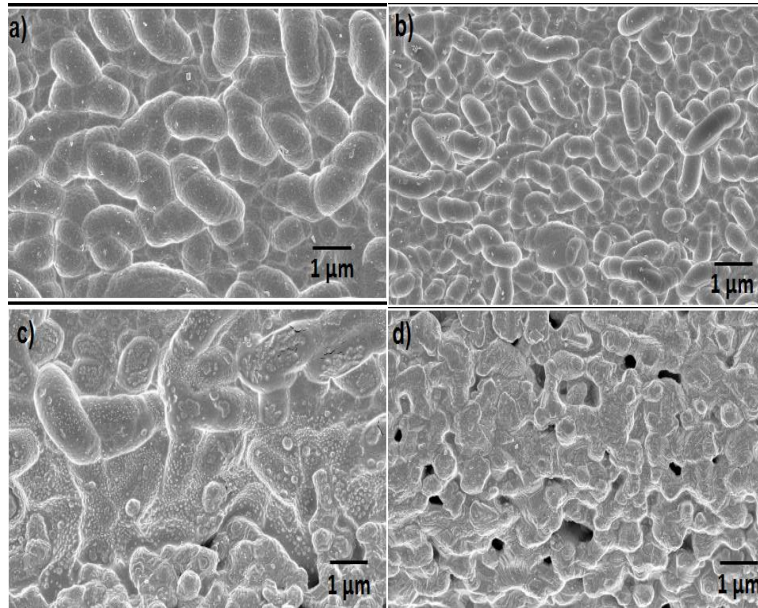


Fig. 2. (a - d) Surface morphology FE-SEM images of MoS₂ coated solar cells of different coating layers for a) C-I, b) C-II, c) C-III & d) C-IV.

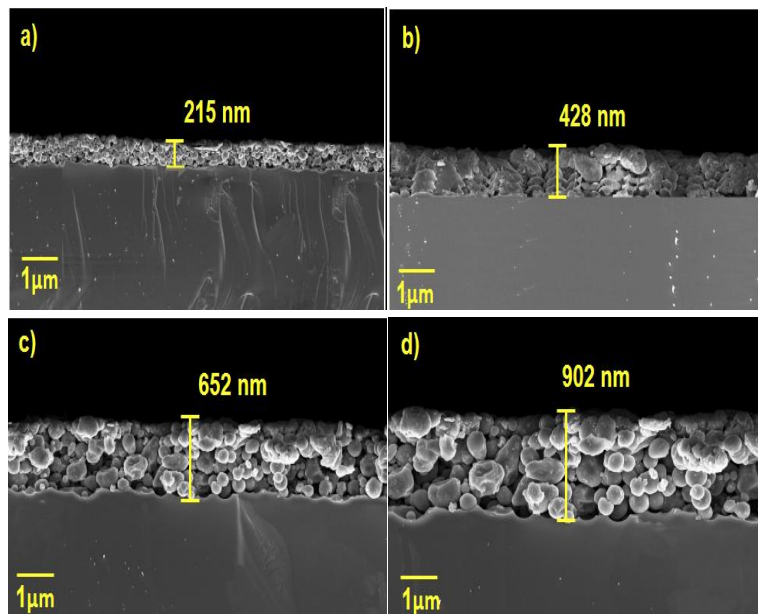


Fig. 3. (a - d) FE-SEM Cross-sectional images of MoS₂ coated solar cells of different coating layers for a) C-I, b) C-II, c) C-III & d) C-IV.

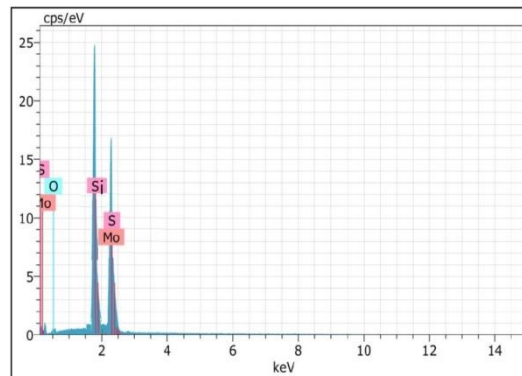


Fig. 4. EDX analysis of C-III coated solar cells.

Compositional and stoichiometry analysis of C-III coated solar cells was carried out by the energy dispersive X-ray spectrometer (EDX) as shown in Fig. 4. and table 2. The EDX analysis confirmed the presence of Mo, S and O elements in the coated MoS_2 film.

Table 2. EDX results of C-III coated solar cells.

| Element | Weight % | Atomic % | Net Int. |
|---------|----------|----------|----------|
| Mo | 17.2 | 5.68 | 93.64 |
| O | 6.57 | 1.30 | 22.08 |
| S | 16.09 | 4.22 | 35.02 |
| Si | 60.14 | 88.8 | 849.26 |

The surface topography of MoS_2 (C-III sample) coated over solar panel has been inspected using Atomic Force Microscopy (AFM). In tapping mode, an area of $10 \mu\text{m} \times 10 \mu\text{m}$ was scanned to evaluate the RMS roughness of MoS_2 film coated solar cells. The three dimensional (3D) and two-dimensional (2D) AFM images of C-III sample are shown in Fig. 5. (a & b). From figure, it is clear that the C-III sample of MoS_2 coated surface is uniform.

The RMS roughness for MoS_2 deposited over solar cells was estimated using standard software. The RMS roughness values are 98, 86, 64 and 53 nm for C-I to C-IV layers of coatings, respectively. The surface uniformity and smoothness is highly preferred parameter to minimize the reflection losses, because the rough surface induces scattering of light [19].

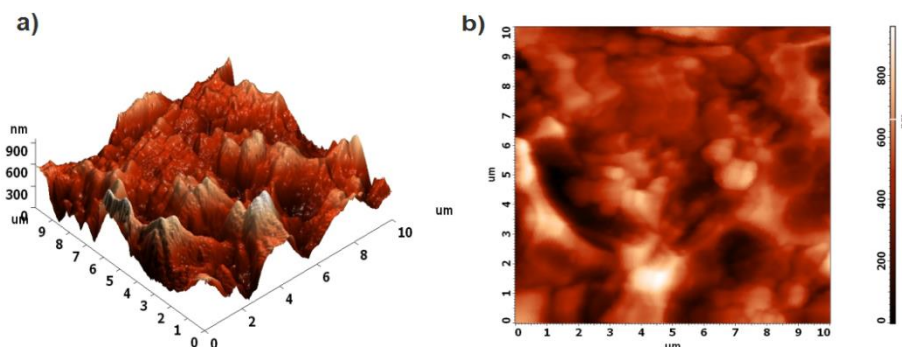


Fig. 5. AFM (3D & 2D) images of C-III coated solar cells.

The optical transmittance and reflectance spectra of MoS_2 thin films coated on solar cells are shown in Fig. 6. (i & ii), which illustrates that the coated films are highly transparent in the

UV visible region at 300 to 800 nm. From the Fig. 6. (i & ii), it is confirmed that there is maximum transmittance (upto 85 %) and minimum reflection (upto 12 %) for C-III coated solar cells. It is also observed that there is increase in transmittance of light and the reflection rate decreases while varying thickness of coating from C-I to C-III. On the other hand further increase in thickness, the transmittance decreases and reflectance increases at C-IV coating layer. This clearly indicates the influence of optimizing coating thickness and coating efficiency. The reduction of transmittance percentage at C-IV coating layer is due to the increase in coating thickness, which restricts the light to reach depletion layer of solar cell. Hence, there is a high scattering of light at the solar cells substrate [20].

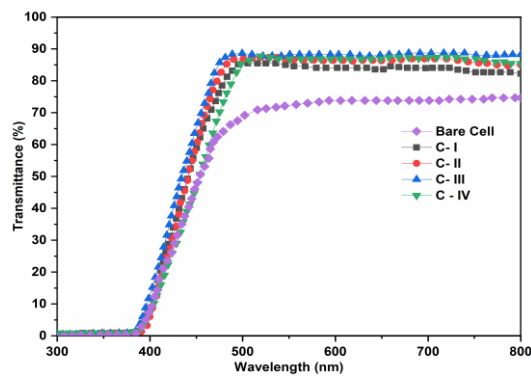


Fig. 6. (i) Optical transmittance of MoS_2 coated solar cells.

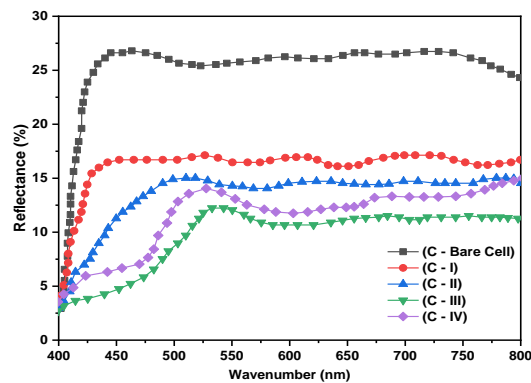


Fig. 6. (ii) Optical reflection of MoS_2 coated solar cells.

The resistivity (ρ) of the bare cell and MoS_2 coated silicon solar cell with different coating layers are depicted in Fig.7. From Fig.7, it is a clear evident that the deposition of layer with the C-III coating exhibits a considerable decrease in resistivity of $2.78 \times 10^{-3} \Omega\text{-cm}$ compared to the pure solar cell of $8.73 \times 10^{-3} \Omega\text{-cm}$. The decrease in resistivity of MoS_2 coated solar cells may be due to the presence of Mo and S concentration. The decrease in resistivity associated with the increase in electrical conductivity of solar cells is analogous to the earlier literature [2, 18]. Further increase in coating thickness to C-IV layer there is subsequent increase in resistivity of $3.02 \times 10^{-3} \Omega\text{-cm}$. The increase in resistivity can be attributed to the coating thickness of solar cell [18, 21, 22].

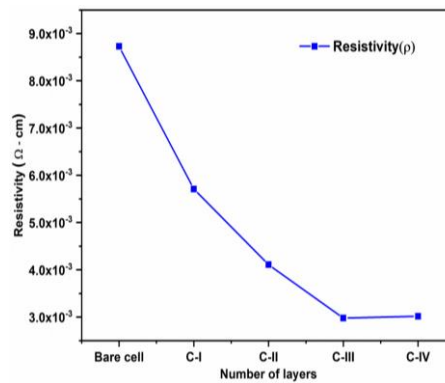


Fig. 7. Resistivity of MoS₂ coated solar cells.

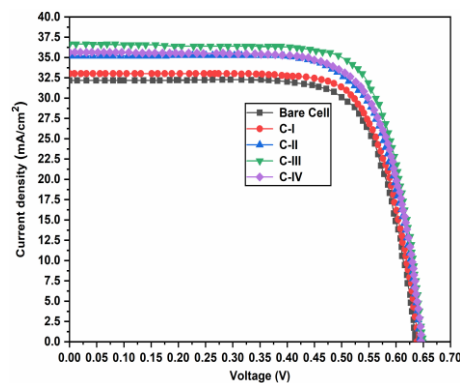


Fig. 8. I-V Plot of MoS₂ coated solar cells under open source environment.

The performance analysis of uncoated and MoS₂ coated solar cells were conducted under both open source environment and controlled source environment in terms of power conversion efficiency (PCE). I -V plot of the bare cell and MoS₂ coated solar cell at open source environment are shown in Fig. 8. The readings were taken by placing solar panel under the sun at 12.30 p.m. The PCE of bare cell and MoS₂ layer coated solar is calculated from I-V plot and the values are shown in Table 3. It is clear that MoS₂ coated silicon solar cell provides better short-circuit photocurrent density (J_{sc}) and open-circuit voltage (V_{oc}) compared to the bare cell indicating the better performance of MoS₂ coating. Particularly, C-III layer of coating displayed a maximum PCE of 17.40 % compared to the bare cell with 14.88 %. Moreover, rising the coating time leads to a drop in J_{sc} value with a successive reduction in PCE. The decrease in PCE at C-IV layer of coating may be due to the increased coating thickness that reduces the transmittance of light to the depletion layer of solar cell.

Table 3. I -V performance at open source conditions.

| Solar cell | V_{oc} (V) | J_{sc} (mA/cm ²) | Fill Factor (%) | PCE (%) |
|------------|--------------|--------------------------------|-----------------|---------|
| Bare cell | 0.631 | 32.0 | 75.9 | 14.88 |
| C-I | 0.633 | 32.9 | 76.1 | 15.37 |
| C-II | 0.639 | 35.1 | 76.89 | 16.62 |
| C-III | 0.648 | 35.9 | 77.0 | 17.40 |
| C-IV | 0.639 | 35.4 | 76.8 | 16.89 |

Fig. 9 shows the solar cells efficiency (I–V curves) of MoS₂ layer coated and bare silicon solar cells under closed controlled environment illuminated by 1000 W/m² neodymium bulb light radiation. Similarly, the PCE of bare cell and MoS₂ layer coated solar cell is calculated from the I–V plot and described in Table 3. The bare silicon solar cell generates PCE of 15.87 % ($V_{oc} = 0.632$ V, $I_{sc} = 33.52$ mA/cm², FF = 75.2 %). As a result, C-III layer coated solar cell displays better PCE of 19.23 % ($V_{oc} = 0.645$ V, $J_{sc} = 38.51$ mA/cm², and FF = 76.8 %). Therefore, high J_{sc} and V_{oc} of MoS₂ layer coated solar cells lead to an increase in PCE from 15.87 to 19.23 %. The C-III layer coated solar cell gives superior PCE compared to C-I, C-II and C-IV layer of MoS₂ coated and bare solar cells. Furthermore, the increase in coating thickness of C-IV layer coated silicon solar cell contributes to a drop in J_{sc} and V_{oc} with a simultaneous decline in PCE as confirmed in Table 4 and Fig. 9.

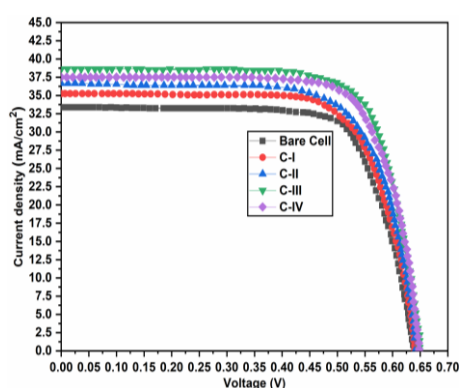


Fig. 9. I-V Plot of MoS₂ coated solar cells under closed controlled source environment.

Table 4. I-V performance at closed controlled source conditions.

| Solar cell | V_{oc} (V) | J_{sc} (mA/cm ²) | Fill Factor (%) | PCE (%) |
|------------|--------------|--------------------------------|-----------------|---------|
| Bare cell | 0.632 | 33.52 | 75.2 | 15.87 |
| C-I | 0.634 | 35.11 | 76.2 | 16.93 |
| C-II | 0.635 | 36.77 | 76.3 | 17.59 |
| C-III | 0.645 | 38.51 | 76.8 | 19.23 |
| C-IV | 0.642 | 37.21 | 76.6 | 18.19 |

Fig. 10 & 11 depicts the temperature analysis of (a) pure and MoS₂ layer coated solar cells (b) C-I, (c) C-II, (d) C-III and (e) C-IV under open environment source and closed controlled environment source respectively. It is seen that the efficiency of solar cells decreases with the increase in temperature. IR thermal imaging technique is used to find the temperature of solar cell for both the conditions. Based on the results, C-III layer coated cells exhibited minimum cell temperature under open environment source (37.5 °C) and closed controlled environment source (52.5 °C) compared to other coated layers and bare solar cell. The improved light scattering increases heat flux of solar cells and thus reduce the transparency of ARC. Therefore, minimum cell temperature considerably improves the PCE of silicon solar cells. Hence, it is clear that MoS₂ layer acted as an excellent ARC material for improving the PCE.

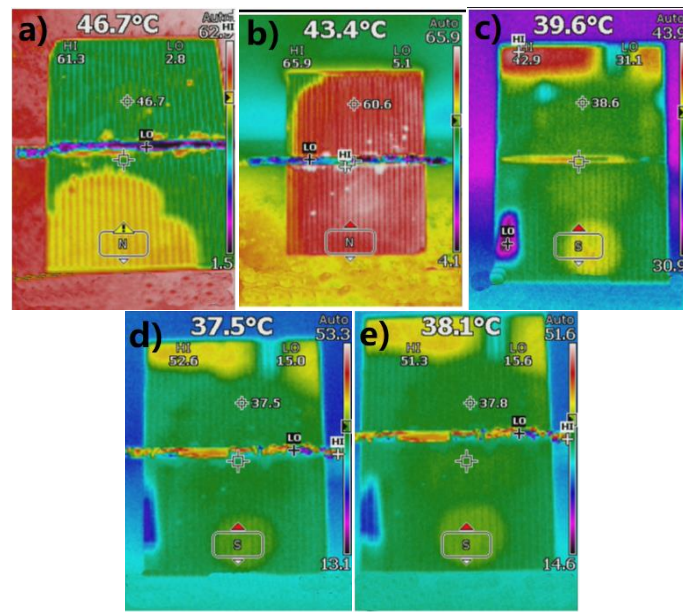


Fig. 10. Open environment condition temperature analysis of a) bare cell & MoS₂ layer coated solar cells b) C-I, c) C-II, d) C-III and e) C-IV.

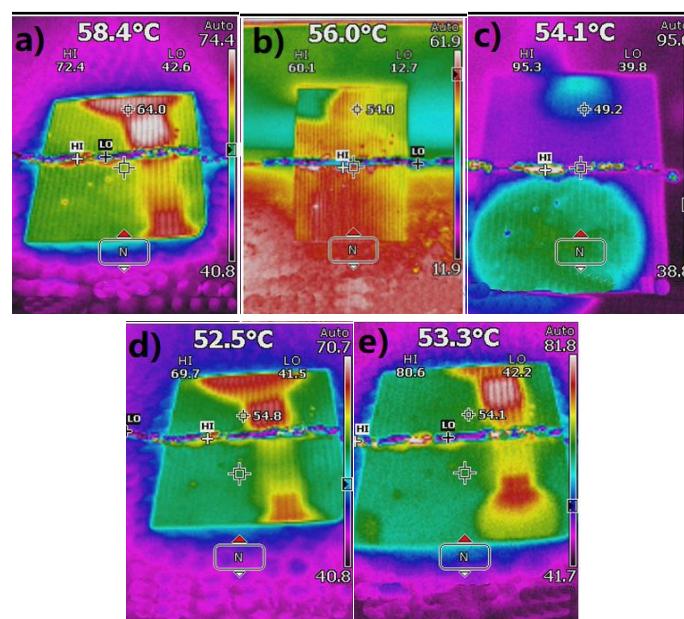


Fig. 11. Closed controlled environment condition temperature analysis of a) bare cell & MoS₂ layer coated solar cells b) C-I, c) C-II, d) C-III and e) C-IV.

4. Conclusions

MoS₂ was coated layer by layer on solar cell substrate through spin coating technique. The Miller indices (002), (100), (101), (102), (103), (106), (105), (106), (110), (008) and (108) generated through XRD results are well matched with MoS₂ crystal structure. From FE-SEM cross-sectional analysis, the thickness of MoS₂ nanolayer is depicted such as 215, 428, 652 and 902 nm for C-I, C-II, C-III and C-IV layer coated samples, respectively.

The C-III layer coated solar exhibits maximum transmittance of 85 % and minimum reflection of 12 % as compared to pure solar cell and other coated layer samples. Polycrystalline solar cell with C-III layer ARC expressed higher PCE at both open condition (17.40 %) and closed condition (19.23 %). The considerable improvement in performance of C-III layer coated solar cells might be associated with the re-orientation of morphological structure, optical and electrical properties and temperature characteristics of MoS₂ layer on silicon solar cell substrate.

Acknowledgements

The authors are thankful to the management of Kongu Engineering College, Perundurai, Erode for providing necessary research facilities.

References

- [1] J. M. Tour, C. Kittrell, V. L. Colvin, *Nature materials* **9**(11), 871 (2010).
- [2] G. V. Kaliyannan, S. V. Palanisamy, R. Rathanasamy, M. Palanisamy, N. Nagarajan, S. Sivaraj, M. S. Anbupalani, *Journal of Electronic Materials* **49**(10), 5937 (2020).
- [3] H. Hanaei, M. K. Assadi, R. Saidur, *Renewable and Sustainable Energy Reviews* **59**, 620 (2016).
- [4] A. S. Sarkin, N. Ekren, Ş. Sağlam, *Solar Energy* **199**, 63 (2020).
- [5] J. Wang, C. Yang, Y. Liu, C. Zhang, C. Zhang, M. Wang, J. Zhang, X. Cui, R. Ding, Y. Xu, *RSC advances* **6**(30), 25191 (2016).
- [6] Z. Lu, Q. Yao, *Solar Energy* **81**(5), 636 (2007).
- [7] S. Khan, H. Wu, C. Pan, Z. Zhang, *Research Reviews: Journal of Material Science* **5**, 36 (2017).
- [8] J. Kischkat, S. Peters, B. Gruska, M. Semtsiv, M. Chashnikova, M. Klinkmüller, O. Fedosenko, S. Machulik, A. Aleksandrova, G. Monastyrskyi, *Applied optics* **51**(28), 6789 (2012).
- [9] G. Hensch, J. Deubener, *Solar Energy* **86**(3), 831 (2012).
- [10] M. Z. Pakhuruddin, Y. Yusof, K. Ibrahim, A. A. Aziz, *Optik* **124**(22), 5397 (2013).
- [11] V. Pawar, P. K. Jha, S. Panda, P. A. Jha, P. Singh, *Physical Review Applied* **9**(5), 054001 (2018).
- [12] D. Chen, *Solar Energy Materials and Solar Cells* **68**(3-4), 313 (2001).
- [13] S.-Y. Lien, D.-S. Wu, W.-C. Yeh, J.-C. Liu, *Solar Energy Materials and Solar Cells* **90**(16), 2710 (2006).
- [14] A. Uzum, M. Kuriyama, H. Kanda, Y. Kimura, K. Tanimoto, H. Fukui, T. Izumi, T. Harada, S. Ito, *International Journal of Photoenergy* **2017**(1), 1 (2017).
- [15] J. Yoo, J. Lee, S. Kim, K. Yoon, I. J. Park, S. Dhungel, B. Karunakaran, D. Mangalaraj, J. Yi, *Thin Solid Films* **480**, 213 (2005).
- [16] G. V. Kaliyannan, S. V. Palanisamy, M. Palanisamy, M. Subramanian, P. Paramasivam, R. Rathanasamy, *Materials Science-Poland* **37**(3), 465 (2019).
- [17] G. V. Kaliyannan, S. V. Palanisamy, E. Priyanka, S. Thangavel, S. Sivaraj, R. Rathanasamy, *Materials Today: Proceedings* (2020).
- [18] G. V. Kaliyannan, S. V. Palanisamy, M. Palanisamy, M. Chinnasamy, S. Somasundaram, N. Nagarajan, R. Rathanasamy, *Applied Nanoscience* **9**, 1427 (2019).
- [19] M. Faraj, K. Ibrahim, M. Eisa, M. Pakhuruddin, M. Pakhuruddin, *Optoelectron, Adv. Mater.* **4**, 1587 (2010).
- [20] G. V. Kaliyannan, S. V. Palanisamy, R. Rathanasamy, M. Palanisamy, S. K. Palaniappan, M. Chinnasamy, *Journal of Materials Science: Materials in Electronics* **31**(3), 2308 (2020).
- [21] H. Du, M. Lv, J. Meng, W. Zhu, *Applied optics* **55**(34), D115 (2016).
- [22] Y. Liu, Y. Li, H. Zeng, *Journal of Nanomaterials* **2013**, 1 (2013).